



Acquisition and analysis of greyscale data from stalagmites using ImageJ software

Sebastian F M BREITENBACH^{1,*} and Norbert MARWAN²

¹ Northumbria University, Department of Geology and Environmental Sciences, Newcastle upon Tyne, NE1 8ST, UK.

² Potsdam Institute for Climate Impact Research (PIK), Member of the Leibniz Association, Telegraphenberg A 31, 14473 Potsdam, Germany.

and

Institute for Geoscience, University of Potsdam, 14476 Potsdam, Germany.

*Correspondence: Sebastian F M Breitenbach [sebastian.breitenbach@northumbria.ac.uk]

Abstract: To reconstruct past climate conditions from speleothems, palaeoclimate researchers utilize a variety of advanced but expensive methods, including various stable isotope ratios and trace element analyses. Greyscale changes can be related to growth and matrix density variations in stalagmites, which in turn are probably dependent on drip rate and dripwater Ca-supersaturation, among other factors. Greyscale analysis is particularly helpful where annual layers are found in stalagmites as the greyscale data can be used to build layer-counting chronologies, similar to varve counting in lacustrine and marine sediments. Greyscale information can further be used as a valuable palaeoclimate proxy. Depending on stalagmite growth rate a spatial resolution of less than five micrometres can be obtained, which might translate to seasonal temporal resolution. Here, we present a low-cost and high-resolution method for acquisition and analysis of greyscale data from speleothems by means of the free ImageJ software. We show how greyscale data can be acquired and visualized and describe how proxy time series can be constructed and proxy record uncertainties estimated using numerical methods. Finally, we provide an example for the application of ImageJ for greyscale analysis on stalagmites. The methodology outlined might be of use to geoscientists working on laminated sediments, and speleothems in particular.

Keywords: greyscale analysis; layer counting; palaeoclimate; palaeoenvironment; proxy data; seasonal growth; stalagmite chronology.

Received: 01 June 2023; **Accepted:** 23 July 2023.

Introduction

Recent decades have seen an astonishing rise in the use of speleothems as palaeoclimate archives, because these chemical sediments offer precise and accurate absolute chronologies as well as a multitude of proxy information (Fairchild *et al.*, 2006; Henderson, 2006; McDermott, 2004; Kennett *et al.*, 2012; Ridley *et al.*, 2015; Wong and Breecker, 2015; Baldini *et al.*, 2021). The complex interactions between the hydrochemistry and crystallography in the soil–host rock–stalagmite system complicate interpretation of geochemical proxy data in terms of climate variations. An approach to overcome this problem is to establish multi-proxy records, where different proxies allow for a deeper understanding of the studied system (see Baldini *et al.*, 2021, and references therein). Where elements or other highly resolved proxies can be linked directly to seasonal environmental changes like infiltration and prior carbonate precipitation, these can be used to develop layer-counting chronologies (e.g., Smith *et al.*, 2009). However, financial constraints often limit the wider application of such geochemistry-based approaches. Thus, it is appropriate to outline low-cost methods that allow the acquisition of proxy data that contain detailed information on (palaeo-)environmental dynamics.

Whereas some researchers have used greyscale analyses for speleothem-based palaeoclimate reconstructions (Genty and Quinif, 1996; Niggemann *et al.*, 2003; Webster *et al.*, 2007;

Jex *et al.*, 2010; Boch *et al.*, 2011; Hopley *et al.*, 2018; Louys *et al.*, 2022;), we find that in speleothem science researchers seem not yet to have taken full advantage of digital image analysis for the acquisition of palaeoclimate and palaeoenvironmental information. Greyscale refers to the amount of light recorded as shades of grey in a pixel of an image, i.e., it represents light intensity in that pixel. A grey value of zero means the pixel is black, while higher values refer to increasingly whiter pixels (in 8-bit images a grey value of 255 is white).

Members of the aquatic palaeoclimate research community, investigating marine and lacustrine sediments, have long made use of density and greyscale variation to characterize and measure annual laminations (varves) (Pike and Kemp, 1996; Rodbell *et al.*, 1999; Nederbragt and Thurow, 2001; Marwan *et al.*, 2003; Patterson *et al.*, 2007; Ebert and Trauth, 2015; Oriani *et al.*, 2022). Similarly, digital methods have long been used to extract palaeoenvironmental information for detailed tree-ring studies and the tree-ring research community has developed a range of software tools for this purpose (see for example, McCarroll *et al.*, 2002; Divya and Kaur, 2021). Some of these tools have been applied successfully to improve stalagmite chronologies (e.g., the TSAP Win software, Riechelmann *et al.*, 2019a). In combination with U/Th dating, floating chronologies based upon layer counting can be anchored, and the age uncertainties of speleothem-based time series can be reduced (Dominguez-Villar *et al.*, 2012).

Other software tools including WinDendro (Regent Instruments Inc.) or WinGeol (Meyer *et al.*, 2006) allow semi-automatic layer detection and analysis. The latest analytical developments include machine-learning approaches (Sliwinski *et al.*, 2023), which – with ever-improving computing power – might revolutionize fast and reliable extraction of seasonal information from laminated archives. A key issue with many professional software packages is their associated licence costs, which commonly restrict the application of digital analysis to specialized laboratories, beyond the budgets of less-well supported researchers.

An alternative is ImageJ, a powerful Java-based public-domain software (Rasband, 1997–2004) that enables researchers from many fields, including astronomy (McGlynn *et al.*, 2008), microbiology (Schjøtt *et al.*, 2008; Ishino *et al.*, 2009), remote sensing (Balic and Koch, 2009), geology (Fischer *et al.*, 2006), and palaeoclimatology (Raffi *et al.*, 2005; Boës and Fagel, 2008; Thomas and Briner, 2009), to extract the information archived in their diverse samples in a reliable and reproducible way.

Stalagmites vary in isotopic, colour, fabric and crystal density, depending upon a variety of controlling factors, e.g., the presence of organic substances (Shopov *et al.*, 1994; Baker *et al.*, 1996), trace element content (Fairchild *et al.*, 2001, 2006), and Ca-saturation state, growth rate (Gabitov *et al.*, 2012; Frisia *et al.*, 2022), and chemical composition of the dripwater (Frisia *et al.*, 2005, 2022). Speleothem fabrics provide a rich archive of information about environmental conditions at the time of their formation (Frisia, 2015), the details of which are well beyond the scope of the present study.

In this study we do not provide a comprehensive discussion of the various physico-chemical parameters that can affect speleothem crystallization and fabrics. Instead, we focus on the extraction of information on growth changes linked to carbonate precipitation rate and crystal density, which allow us to construct layer-counted chronologies, and/or gain insights into seasonal to multi-annual environmental dynamics. Complex relationships between stalagmite growth laminae and climate in an Alpine cave are discussed by Boch *et al.* (2011). Connecting microclimatic data and geochemical monitoring they were able to disentangle the climatic parameters that lead to lamination changes. However, the processes producing annual laminae in a stalagmite are likely to differ depending upon local environmental conditions at each study site. Grey values, measured in speleothems along the growth axis, are likely to change with matrix density (Genty and Quinif, 1996). Lower grey values commonly correspond to high CaCO₃ matrix density, whereas higher grey values are related to higher matrix porosity (low density). In reflected-light scans, dense CaCO₃ with a microcrystalline structure often appears more transparent but is darker in scanned images because of the samples' lower reflectance. Porous crystals generally appear rather opaque, leading to brighter grey values, as the scanning light reflection increases. Factors controlling the matrix density are commonly related to changes in stalagmite growth rate, which in turn depend on the soil pCO₂, the hydrochemistry in the overlying host rock, and ultimately (cave) climate (Fairchild and McMillan, 2007). Thus, stalagmite greyscale data can provide a powerful proxy for hydrochemical, and hence palaeoenvironmental, variability in the past.

We note that images obtained using other optical methods, such as petrographical and fluorescence microscopy, can be scrutinized in a similar fashion to the methods outlined here (Baker *et al.*, 1993; Baker *et al.*, 1996; McGarry and Baker, 2000; Baker *et al.*, 2008; Hopley *et al.*, 2018). Microscopic techniques allow even higher (even sub-micron level) resolution, but come with different complexities, including the need for thin sections and advanced equipment. Importantly, petrographical

microscopy uses transmitted rather than reflected light, which means that the interpretation of low and high grey values differs to that of grey values obtained using reflected light. Another potential issue that needs to be recognized and corrected is the potential distortion of microscopic images (i.e., changes of the shape of an image such that the true sample geometry appears altered). Flatbed scans have the light source always vertically above the object, rendering distortion insignificant. If these and other factors are considered carefully, grey values from such images can be analysed in the same way as described here and can give extremely detailed insights into sub-annual to multi-annual environmental dynamics.

Some stalagmites do not exhibit clearly visible banding, or observed layers are related to inclusion of detrital (silt/clay) material deposited during erratic flood events rather than to seasonal growth changes (Dasgupta *et al.*, 2010; Louys *et al.*, 2022) and this can prove challenging for greyscale analysis as described below. Where grey values vary regularly on a seasonal scale, greyscale analysis can help to establish a chronology based on layer counting. An important precondition for the formation of (seasonal) layers is that the hydrological regime of a cave reacts fast enough to seasonal environmental changes, and that the carbonate deposition rate is appropriately high. A counting chronology (similar to varve chronologies in lake sediments, e.g., Mangili *et al.*, 2007) should ideally be confirmed by independent methods, such as U/Th dating. An example of a speleothem record based on a combined layer-counted and U/Th chronology for a stalagmite is provided by Myers *et al.* (2015).

Below, we outline how ImageJ can be used as a low-cost yet effective digital tool to acquire greyscale values from stalagmites to construct layer-counting chronologies and proxy time series that can inform on seasonal changes in carbonate deposition during stalagmite formation.

Sample preparation setup

The described extraction and analysis of greyscale data is based on grey values observed in a stalagmite. As mentioned, grey values vary with changes in carbonate density, crystallographic fabrics, and organic content (if UV or confocal data are used), which depend on environmental conditions during carbonate deposition. The grey values are extracted from images of a stalagmite surface obtained using a flatbed scanner, with the scan image being based on reflected, rather than transmitted, light. This is a significant difference to petrographical thin section analysis, where transmitted light is used (e.g., Aharon *et al.*, 2006).

Prior to scanning, a speleothem surface is prepared by cutting a stalagmite in half along its growth axis, normally with a rock saw or a wire saw. Depending upon the smoothness of the result, the cut surface might require polishing. This normally requires access to a laboratory equipped with a polishing table, and appropriate experience in polishing relatively soft rocks, though do-it-yourself solutions using sanding and polishing tools have been tested successfully. In some cases high porosity renders a sample unsuitable for polishing, because carborundum paste becomes trapped in the pores and interstitial spaces between crystals. The trapped paste is difficult to remove (even using ultrasonic methods) and it can bias the grey shading of the sample. Dry sandpaper and handheld drills with polishing attachments help in some instances, and a sufficiently smooth surface might even be obtained without polishing, simply by using a rock saw.

To obtain high-quality scans the sample surface should be free of scratches from cutting, because these would appear as spurious grey values within the scan. Samples that exhibit dense crystal growth and horizontally deposited laminae are more likely to show regular seasonal growth changes and are ideally suited for greyscale analysis.

Greyscale data acquisition

Required instrumentation and software

A flatbed scanner with a scanning resolution of 3600 dpi (dots per inch) or higher is recommended for greyscale data acquisition. ImageJ is freely available online [<https://rsb.info.nih.gov/ij/>] and runs on most operating systems. For pre- and post-processing of the scanned images, image editing software (such as AdobePhotoshop® or Gimp) might prove useful, although ImageJ itself supports advanced image manipulation. The extracted data can be explored further using any spreadsheet or data analysis software. Data analysis and visualization can be achieved using Goldensoft Grapher®, Octave, MATLAB™, Python, Julia, or similar software. MS Excel® is of only limited use when large data series are gathered and need to be illustrated or if more-complex data analysis is necessary.

Considerations for scanning

First, a decision has to be made as to which spatial resolution is actually needed. An image of a polished stalagmite surface, scanned at 4800 dpi gives a spatial resolution of 5.29µm/pixel (Fig.1). Higher resolution is possible but renders image handling more cumbersome, especially when using long scanned sections.

As mentioned above, far higher (sub-micrometre) resolution can be achieved using microscopic images (e.g., when studying UV fluorescence) (Baker *et al.*, 1993; Hopley *et al.*, 2017).

The scan resolution should thus be adjusted depending on the average growth rate of the sample, typically in the range of 50µm/year to 200µm/year (Baldini *et al.*, 2021). If, for example, a stalagmite grew 15µm/year a scan with 1200 dpi resolution would result in 7.1 pixels (samples) per year, which would make it difficult to identify annual growth bands (Table 1, Fig.2). Using a scan resolution of 3200 dpi on the same sample would give about 19 samples per year, i.e., roughly three-weekly resolution, which would suffice for annual layer identification even if growth rates vary slightly.

Submerging the stalagmite in a water-bath on the scanner glass can help to enhance contrast and brightness. Attention must be paid not to trap air bubbles between glass and stalagmite. To avoid water entering the scanner, plasticine or a reusable adhesive such as Blu Tack®, can be used to model a dam around the sample on the scanner. If subsequent geochemical investigations are planned, the use of high-purity (or at least distilled) water is recommended. Covering the sample with an opaque plastic or cardboard box prevents unwanted light scattering.

An 8, 16, or 32-bit greyscale scan can then be taken at the desired spatial resolution, whereas the pixel depth (the bit-number) defines the number of grey levels, i.e., 8-bit has 256 grey levels (usually sufficient), 16-bit 65,536 grey levels, and 32-bit more than 4 billion. The image should be saved as a .tiff file. Image formats that induce data loss during compression (e.g., .jpg) are not recommended. It is good practice to include a scale in the scan, and to record the dpi setting used during scanning.

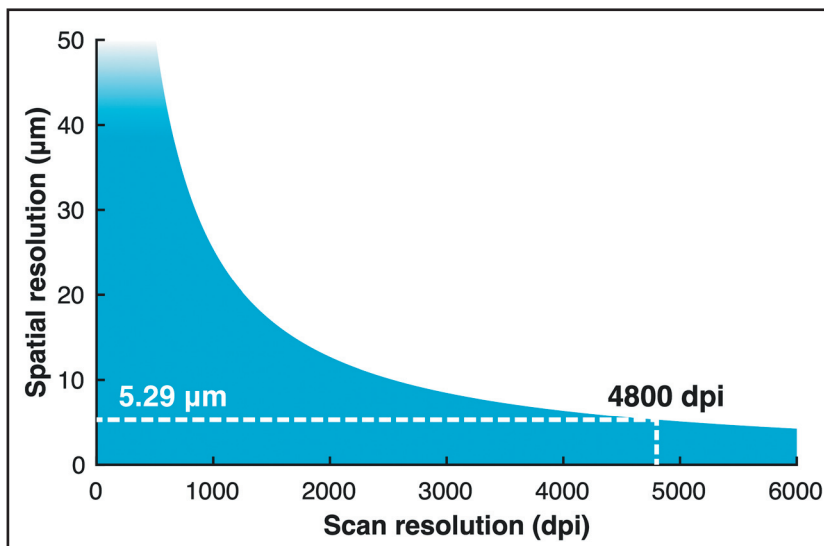


Figure 1: Relationship between the scan resolution in dpi and the spatial (pixel) resolution. For example, at 4800 dpi scan resolution, the spatial resolution of greyscale data will be 5.29µm (dashed line).

Scan resolution (dots per inch)	Pixel size (µm)	Stalagmite growth rate (µm/year)	Samples per year	Sampling time
4800	5.29	200	37.8	9.65 days
		150	28.4	12.9 days
		50	9.5	38.4 days
		10	1.9	6.8 months
		5	0.95	13.7 months
3200	7.94	200	25.2	14.5 days
		150	18.9	19.3 days
		50	6.3	1.9 months
		10	1.3	9.2 months
		5	0.6	1.7 years
1200	21.17	200	9.4	1.3 months
		150	7.1	1.7 months
		50	2.4	5.1 months
		10	0.5	2.1 years
		5	0.2	4.2 years

Table 1: Temporal resolution achieved at different scan resolutions and selected stalagmite growth rates.

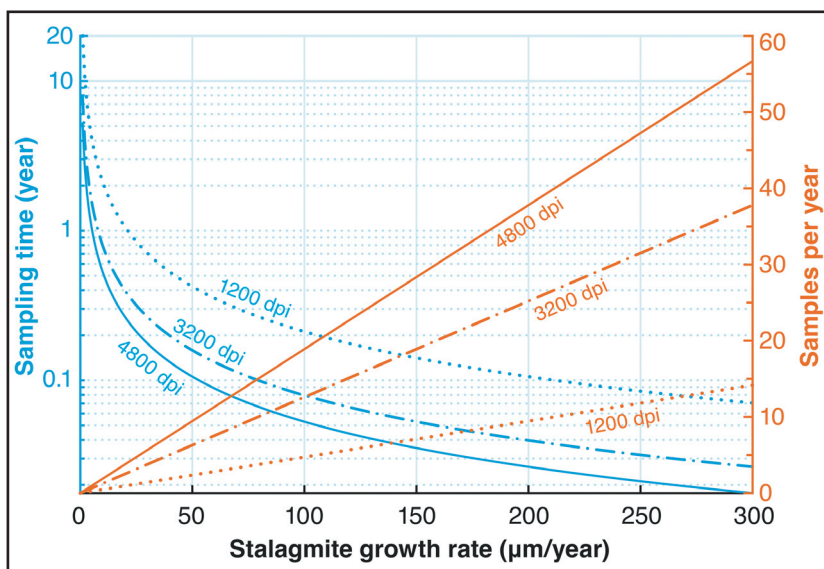


Figure 2: Relationship between stalagmite growth rate, sampling time, and obtainable number of samples/year at selected scan resolutions.

Working in ImageJ

The scan image obtained can be opened in ImageJ, and contrast and brightness can be adjusted on-screen for better visibility (with no effect on the image; all grey values will be recovered). Ensure that a working copy of the image is used, and keep the original scanned image in a different folder or under a different and unmistakable file-name, to avoid accidental manipulation of the original image. It is also strongly advised that a version control system such as GIT is employed to monitor progress and maintain backups of previous stages of the work.

To link grey values to a metric distance rather than to a number of pixels, the measurement scale needs to be defined using the set scale tool in ImageJ (Analyze > Set scale), which relates a pixel distance to a known distance (e.g., a ruler scanned together with the sample). For example, a scan of 4800 dpi corresponds to 188.89 pixel per 1000 μ m.

The easiest way to extract a greyscale track (a single line) is to select the Line Tool (in ImageJ's main menu) and draw a line along a transect of choice (the line can also be 'segmented' or 'freehand' to allow easier tracking of the growth axis). The selected line can be thickened to get average values of a range of pixels along the line (Image > Adjust > Line Width). Widening the track can reduce noise because the recorded grey values are less likely to stem from random particles or holes on the trackline. We recommend a trackline width of between 7 and 30 pixels, although this is highly dependent upon sample characteristics, and ideally should be tested for each individual sample.

To ensure reproducibility of the analysis by other researchers, the trackline should be saved as a region of interest (ROI) in the ROI Manager (this can be found in Analyze > Tools > ROI Manager). This supports the saving of a ROI file (ROI Manager: More > Save), extraction of the coordinates of the trackline (ROI Manager: Properties > List coordinates), and the re-use of previously defined tracks (ROI Manager: More > Open), thus allowing the reproduction of results. We define a track as a single line along the stalagmite growth axis (perpendicular to growth layers, Fig.3) that is stored in a **track.csv** file. A number of tracks can be stacked into a profile (profile = n tracks).

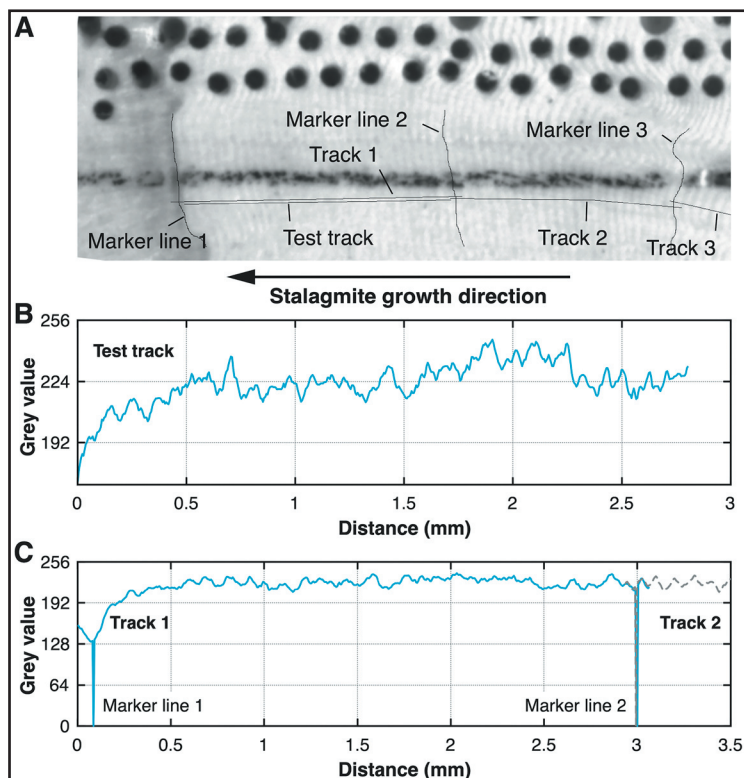


Figure 3: Plotting a grey value profile for selected tracklines. (A) marker lines and tracklines can be used to build a profile of n tracks. (B) A test track shows the quality of the grey profile before crossing the marker lines and fixing of the track. This test track can repeatedly be plotted to find the most suitable track. The chosen track is then extended to cross the marker lines and fixed on the image by **Ctrl+D**. (C) The track crosses the marker lines 1 and 2 (indicated as very low grey values) and can be used to tie further tracks (track 2, grey dashed line). The grey values can now be saved as, e.g., **track.csv**.

In ImageJ, the grey values can be plotted against distance using the key combination of **Ctrl+K**. If the scale has not been set, the pixel number will be shown instead of the metric distance. The grey values can be saved as **track.csv** output (in the window with the grey values under Data > Save), and the drawn trackline can be added permanently on the image using the key combination **Ctrl+D** (ensure that the changes are made on a working copy and not on the original scan, because this line is added permanently to the image).

The procedure outlined above is useful for single tracks or for short intervals of interest. For more complex analyses, especially on samples characterized by changes in growth axis angle, some refinements of the procedure might be desirable. If a long transect, including changes in growth direction is planned, it is recommended to draw marker lines (with a width of 1 pixel) along certain distinct features parallel to selected growth layers, dating samples or similar points that serve as stratigraphical markers (Fig.3A) before starting the actual profiling of tracklines. These marker lines help in the stacking of multiple tracklines into a combined master profile, and to define the distances of features of interest (e.g., visible hiatuses, dating samples, changes in growth axis, etc.) along the master profile. For maximum accuracy, each track should be bracketed by a starting marker and an end marker line. For a larger project we recommend initial preparation of a sample scan with all required marker layers. After all marker lines are defined, the entire (stacked) profile can be developed and drawn over the entire length of interest. It might be useful to record the marker lines in the ROI Manager for archival purposes.

Because the grey values are black (i.e., zero or near-zero) at the position of the marker lines (Fig.3C), their position can be identified readily on the transect of interest. Since the marker line grey values are added artificially, subsequently they should be replaced by either the true grey values (to avoid gaps in the stacked profile) or as a gap in the profile (commonly the loss of 1 pixel of information is not significant for the reconstruction). The grey values beneath the marker lines must be determined manually. If the tracklines have been saved as ROI the track can be redrawn without the marker lines to obtain the grey values formerly beneath them.

Whereas the marker lines are kept as thin as feasible to minimize any data gaps, the thickness of the trackline (Image > Adjust > Line Width *or* Properties > Width if using the ROI Manager) may be adjusted to avoid unwanted noise (as mentioned above). Commonly a trackline thickness of 15 to 30 pixels reveals growth patterns more accurately, and the grey values are more representative compared to single-pixel tracklines (depending upon scan resolution and sample characteristics). In each case the ideal trackline thickness should be evaluated manually, because growth and fabric characteristics vary from sample to sample.

In a stacked profile, the end marker of the first track serves also as the start marker for the second track and so on. This strategy allows the user to adjust the track to follow changes in the direction of the growth axis, or to avoid holes, cracks, or other features that are unrelated to seasonal growth patterns. When starting to record tracklines, a line can be created to follow the profile of choice. It is recommended that initially a track is drawn between two markers, without actually crossing the marker lines, and that the track quality is evaluated using **Ctrl+K** (Fig.3B), before extending the trackline across the marker lines for archiving (Fig.3C). This facilitates choice of the most representative transect before the final trackline is drawn and the data are saved in the respective **track.csv** file and ROI.

Before moving on to extract the next trackline, the previous line should be saved as a ROI in the ROI Manager (using the Add button) and fixed on the image, using *Ctrl+D*, for archiving and visualization purposes (strictly speaking, the latter step is not necessary because the ROI ensures precise archiving of all track information). The track and marker lines should be labelled using a consistent and structured scheme to maintain automatic post-processing and reproducibility (e.g., **track_01_year-month-day.csv**; start marker #01). For ease of handling, all tracks should be recorded consistently in the same direction, either from top downwards, or from base upwards.

Once all desired tracks have been recorded and saved, the individual track lengths must be combined in a master track and all individual lengths should be connected and related to ‘Distance from top’, i.e., relative to the apex of the stalagmite. To combine the track distances within a master record, it is simplest to start with the topmost track and proceed in stratigraphical order: track 2 is found below track 1, and track 3 below track 2, etc.

Ideally the position of the first marker line is placed at the top of the stalagmite and defined as 0mm from top, so that the distances of track 1 will then not need to be adjusted. Track 2 distances would then have to be redefined, however, such that all grey values above the top marker line are discarded. The distance of the top marker line of the second trackline is then defined as the distance of the bottom marker line of track 1 and the following distances are added to the first track. In this way, all tracks can be combined into a master record.

If the top of the stalagmite has been defined with a marker line, all distances in tracklines can be adjusted and linked to the top of the stalagmite. This track should be used for all other dating and proxy information – all distances of samples taken from the stalagmite should be measured from the same reference depth (here marker line 1). We define this track as the master record or *reference track* with respect to distances. As stated, all distances should only be either measured directly along this reference track, or projected onto it. Equally important is that this establishes a *datum line*, i.e., a reference point that defines the top of the stalagmite, and this serves as starting point for measuring and recording all distances. This is of great importance for linking proxy distances (e.g., grey values, stable isotopes, etc.) and discrete dating samples in preparation for age–depth modelling.

The raw distance data in a **track.csv** file contains the total length of a greyscale trackline drawn (from the start of that line to the end). This is obviously not the correct (final) distance of the master profile and corrections are necessary as outlined above. The relevant part of a trackline is the distance between the two marker lines; anything above or below is irrelevant for the composite profile and has only been recorded to allow detection of the marker lines. In the **track.csv** file, the low grey value of the marker line can readily be found and the distance of interest extracted. When using an analysis software, these marker lines can be found automatically by applying a threshold. From experience, the threshold can be defined as the 10%-quantile of the original image. Then, values below this threshold in the track’s grey values can be considered as the marker lines.

The values before the start marker and beyond the end marker are discarded from the master composite profile and the raw **track.csv** data are imported into a spreadsheet. To avoid confusion, the spreadsheet should contain a column that contains the name and date of data acquisition of the **track.csv** file, and another column the distance from marker to marker (length of each track). A third column contains the total distance of the stacked composite profile (*n* tracks), and a fourth column contains the grey values.

Alternatively, an analytical scripting software (e.g., MATLAB) can be used, allowing automatic marker detection, merging of the single tracks, and definition of the final total (stalagmite-based) distance (an example MATLAB script **combine_tracks.m** can be found in a linked Zenodo archive: see **Data and code availability** below).

The composite data can now be explored for seasonal growth changes, layer thickness, changes in mean grey values, and layer-counting purposes. To test whether the resulting reconstruction is accurate and representative, a second, parallel profile should be extracted in the same way (see for example Hopley *et al.*, 2018). Based on several (>3) profiles one can also calculate an average layer count and its standard deviation as estimate of counting uncertainty.

Constructing a greyscale time series

Once a composite greyscale profile has been compiled, the main task might be the construction of a time series of grey values that can be scrutinized for environmental signals that forced changes in speleothem growth, and, hence, the grey values. Below, we discuss two ways to construct greyscale time series. First, we give some considerations when building time series via interpolation between points of known age (today mostly obtained via U/Th dating). Secondly, we discuss how layer-counting chronologies can be constructed (e.g., based on grey values).

Henceforth, we refer to the “greyscale record” as the series of grey values based on distances, and to the “greyscale time series” as the grey values based on a timeline.

Interpolation-based chronologies

An established greyscale record can now be plotted against distance along the growth axis of the stalagmite. However, in order to study the greyscale variation as a time series, compare with independent proxy records, or analyse the profile statistically for archived periodic climatic/environmental changes, such as the El Niño–Southern Oscillation (ENSO) or the North Atlantic Oscillation (NAO), an age–depth model is needed to inform construction of a greyscale time series.

To construct such a time series of grey values with an interpolated chronology, at least two fixed dating points must be known along the track (e.g., based on U/Th dates or known historical events that can be identified in the stalagmite). Ages can be assigned to each grey value by interpolation and extrapolation between these dating points using a simple linear model, or more advanced methods like cubic, spline, or piece-wise shape-preserving cubic interpolation. A template analysis script **chronology_with_uncert.m** for various interpolation and extrapolation calculations (working with Octave and MATLAB) can be found in the linked Zenodo archive [see **Data and code availability** below]. A detailed discussion can be found in Breitenbach *et al.* (2012).

Whereas linear interpolation is the best method to use if only two dates are available, this method has the disadvantage that the age model can falsely suggest abrupt growth changes at the dating points, which renders the logic of the resulting age model faulty. This is because growth rate (i.e., the relationship between distance and age) would appear to change exactly where the dating samples have been taken, which is highly unlikely in nature. The growth rate would change either gradually, or somewhere between dating points, rather than at a specific (subjectively chosen) position. Additional disadvantages of linear interpolation, and also of other interpolation methods, are summarized in Scholz and Hoffmann (2011) and Breitenbach *et al.* (2012). Where multiple dates are available, we recommend use of interpolation techniques that provide smooth transitions at the dating points, such as cubic interpolation. Commonly interpolation is also necessary when subsequent time-series analysis requires an equidistant timeline, although novel statistical approaches have been developed in recent years that can handle non-equidistant datasets (e.g., Rehfeld *et al.*, 2011; Ozken *et al.*, 2015). For a useful overview of numerical strategies for time-series analysis see Chapter 9 of Kwiecien *et al.* (2022).

Here, in a first step, we define an equidistant timeline and calculate corresponding distances to this timeline by using the aforementioned interpolation procedure. In a second step, the distance-based greyscale record is interpolated to the equidistant timeline, resulting in a greyscale time series on an equidistant timeline.

The measurements of the distances of grey values (or any proxy for that matter) and (mainly) the corresponding U/Th dates contain uncertainties. Using a simple Monte Carlo simulation (Breitenbach *et al.*, 2012), we can estimate the confidence intervals of the chronology and translate them into confidence interval variations of the grey values themselves. This means that we can estimate what the most likely proxy value is at a given age.

One example: Consider a dating error of $\Delta T = \pm 50$ years and a tiny error in the distance measurement of $\Delta D = 0.02$ mm. Then random numbers, derived from a normal distribution and scaled to the necessary corresponding error ranges, are added to the dates and position values of the dating points. This results in a new and slightly different realization of the age–depth relationship, which is, however, still within the range of the measurement errors. From this new realization, a new chronology for the greyscale profile is calculated. Next, the greyscale record is interpolated to the new timeline. By repeating this procedure many (say 1000) times (Monte Carlo simulation), many new realizations of age–depth relationships and interpolated greyscale records can be obtained. These can then be used to derive a distribution (an ensemble) of grey values for each time point, which allows us to estimate the standard deviation or a pre-selected quantile, mainly the 2.5% and 97.5% quantiles, and, hence, the 95% confidence interval of the greyscale time series. We emphasise that uncertainty estimates of the proxy time series itself (be it grey layers, isotopes, elements or any other) are commonly absent in published stalagmite records. The methodology described above (and in more detail in Breitenbach *et al.*, 2012) and provided in the Zenodo archive (see **Data and code availability** below) can be applied to any proxy and any sedimentary record, as long as the dating uncertainty is well known. The COPRA Toolbox, a free toolbox for Octave and MATLAB, includes this procedure and can be accessed at <https://tocsy.pik-potsdam.de/copra.php>.

Such simulations show that very small errors in the dating can cause rather strong variances in the greyscale time series. This uncertainty should be considered when interpreting the resulting proxy record in terms of past environmental changes.

Building layer-counting chronologies

Once a greyscale record (grey values versus distance) has been established, it might be possible to construct a layer-counting chronology.

In stalagmites a given layer is always older than the next one above it, similar to the innermost tree rings always being the oldest. This fundamental stratigraphical principle underlies our counting exercise where we use the greyscale profile to build a record of counted layers. We define an annual layer as the distance between two adjacent maxima (or two adjacent minima) within the greyscale record, assuming that growth conditions vary at seasonal scale, with environmental conditions in one season producing a denser, darker layer, and another season producing a whiter, more porous layer. A key assumption is that the layers are indeed formed at seasonal scale. Although not all caves support this type of seasonal variability and therefore seasonally variable carbonate deposition, seasonal growth changes have been observed in different climatic settings (Aharon *et al.*, 2006; Johnson *et al.*, 2006; Boch *et al.*, 2011; Myers *et al.*, 2015; Ridley *et al.*, 2015; Baldini *et al.*, 2021). Some stalagmites reveal multiple sub-seasonal (event) layers or missing annual layers (Shen *et al.*, 2013) and it is strongly recommended to verify the seasonal nature of observed layers using an independent dating method, e.g., U/Th dating.

Because radiometric dating methods are commonly associated with larger uncertainties (many years, or even centuries), layer-counting chronologies remain floating, i.e., a layer-counted chronology can be (timewise) moved within the dating uncertainties of the independent dating method. However, the internal (year-to-year) accuracy of a layer-counted interval is commonly far higher than the uncertainties

related to the U/Th chronology. This realization allows new insights into seasonal and interannual environmental dynamics, regardless of the absolute calendar age. Given that two chronologies – layer-counting versus radiometric dating – agree within uncertainties, the annual character of the observed layers and the quality of the counting method are validated. If the annual nature of greyscale cycles is verified, the layer-counting chronology can further help to improve the relative timing and duration of events that might be detected with proxy data. Verification might be provided by observations of modern carbonate deposition (e.g., isotope analysis of monthly deployed watch glasses, Riechelmann *et al.*, 2019b), chronological agreement between U-series dates and layer counts (Dominguez-Villar *et al.*, 2012), or agreement between layer-counted age and events of known age in a sample (Baker *et al.*, 2008).

Whereas the minima or maxima in the greyscale profile allow us to count years, it is impossible to assign the *season* to maximum or minimum grey values without detailed monitoring of microclimate and dripwater chemistry (Baldini *et al.*, 2021; Kwiecien *et al.*, 2022). Thus, the distance between two subsequent maxima (or minima) represents the annual deposition, without unequivocal information on the calendric season. Calculating the distance between the counted grey value peaks, the greyscale profile provides an annually resolved record of growth rate, which in itself can provide valuable environmental information because stalagmite growth rate depends directly upon local environmental conditions (Baldini *et al.*, 2021).

Linking layer counting and U/Th chronologies

Various approaches have been proposed to link layer counting and U/Th chronologies. One method involves minimizing the distance between U/Th data and layer counts through a least-squares fit, as described in detail in Breitenbach *et al.* (2012). To anchor the two chronologies Domínguez-Villar *et al.* (2012) used a linear relationship between the layer-counted chronology and the U/Th chronology, determined through a least-squares fit. Another approach is to assign a common age point to a given depth and use that tie point in both chronologies, without further testing for agreement between layer counting and U/Th results as in the previous methods. The tie point could, for example, be the centre of a U/Th dating sample as implemented by Finestone *et al.* (2022), or an event layer of known age that is used as a reference point for layer counting. These different strategies provide flexibility in linking layer counting and U/Th chronologies and offer insights into the temporal evolution of geological formations, while potential sources of uncertainty are being considered.

Uncertainties inherent to greyscale analysis

A single track along the growth axis might be rather subjective and it might be useful to evaluate the accuracy of the trackline with another parallel one, as mentioned above. Holes or dirt inclusions, etc., in the sample can falsify the grey value information (both greyscale proxy and chronology). Also, as shown nicely by element imaging (Treble *et al.*, 2005), single layers might taper out with growing distance from the central growth axis, up to the extent of disappearance. Such sample characteristics will lead to falsification in a greyscale chronology because either too many or too few layers might be identified and counted. To minimize the impact of these issues, it is useful to adjust the width of the trackline such that it can be considered representative of the stalagmite. We find that a line width of between 7 and 30 pixels is often best to suppress unwanted noise (from, e.g., holes, cracks, or particles) and to extract well-expressed seasonal changes in grey values. The exact width that is best for each line should be tested because it depends upon the characteristics of the sample at hand.

This approach helps to avoid some – though not all – problems that can complicate the extraction of greyscale information. Missing layers (Shen *et al.*, 2013) and crypto-hiatuses (Baldini *et al.*, 2021) will likely remain undetected. It is obvious that the best samples are those displaying quasi-parallel lamination. On the positive side, if agreement between layer-counting and an independent dating method is found, the error resulting from the above-mentioned uncertainties is probably masked by the error of the radiometric dating method.

An example for greyscale analysis

We chose a short section of a stalagmite from northeastern India as an example for greyscale analysis. The entire dataset and the palaeoclimatic interpretation ($\delta^{13}\text{C}$, $\delta^{18}\text{O}$, and greyscale data) of this stalagmite are presented in Breitenbach (2009). Here, we use the greyscale information as an independent chronological tool and as an aridity proxy. We show only a short section of this set of data to illustrate the method outlined above. The 64cm-long stalagmite KRUM-3 originates from the cave Krem Umsynrang, in Meghalaya, northeastern India. This region is characterized by sharply pronounced rainfall seasonality, with >80% of the annual rainfall being delivered between June and October. After being collected in 2006, the laminated aragonitic stalagmite was subsequently analysed using geochemical methods, and has been dated using the U/Th method (for details see Breitenbach, 2009). The cave is overlain by about 40m of sandstone and a thin coal bed.

KRUM-3 greyscale profile

To exemplify the outlined approach, we chose the KRUM-3 section between 16mm to 32mm from the top (Fig.4), that corresponds roughly to track 1 and track 2 in Fig.3A. The unpolished stalagmite slab was scanned in a water bath at 4800 dpi resolution with 8-bit pixel depth, and the grey values were extracted with ImageJ in the way described above. Petrographical microscopy revealed that dense microcrystalline layers are characterized by reduced growth rates. These intervals appear dark in the scan (Fig.4). The layer counting started at the top of the stalagmite with year 2006 AD when the stalagmite was collected.

The profile shows large grey value variations, ranging from 180 to 255. Cycles are clearly visible between the values of approximately 200 and 230. These cycles result from seasonally varying growth rates. Independent information (petrographical observations, higher $\delta^{18}\text{O}$ and $\delta^{13}\text{C}$ values) suggests that darker grey values reflect dry (season) conditions and reduced growth (Breitenbach, 2009). In turn, higher (brighter) grey values reflect wetter conditions during the Indian summer monsoon. The same interpretation of dark and bright layers, as mirroring dry and wet periods respectively, has been proposed by Aharon *et al.* (2006) in speleothems from Niue Island in the southwestern Pacific. Dark bands there were found to be linked to slower carbonate deposition reflecting a restricted dissolved inorganic carbon (DIC) load, whereas brighter layers were formed when increased infiltration led to a higher DIC load and faster crystal growth (Aharon *et al.*, 2006). Whether faster growth occurs during the dry or wet season depends upon several factors, and monitoring is required to establish during which season growth is enhanced or suppressed. For example, in Mawmluh Cave, 1000m higher than Krem Umsynrang, on the Shillong plateau, faster growth (with more-porous and whiter crystals, and higher isotope values) is found in the dry season (Ronay *et al.*, 2019).

Thus, the variability of the grey values serves as a proxy for local hydrological conditions. In northeastern India, the greyscale record obtained reflects changes in summer monsoon intensity. Similarities between the greyscale data and a record of ENSO changes in Peru suggests that hydrological seasonality and monsoon strength are influenced by ENSO dynamics, as also indicated by other studies (Breitenbach, 2009; Myers *et al.*, 2015; Ronay *et al.*, 2019).

Sub-monthly temporal resolution can be obtained where high growth rates are found (in our example we obtain 15 to 20 samples per year because the annual growth commonly exceeds $100\mu\text{m}$). However, periods of reduced growth during dry intervals decrease the sampling to sub-decadal resolution. Such intervals can introduce larger counting uncertainties if the individual layers can no longer be distinguished, leading in turn to disagreement with U-series dating results.

KRUM-3 greyscale layer-counting chronology

The counted interval corresponds to 169 years between U-series dates U8 (405 ± 7 yrs BP) and U32 (574 ± 5 yrs BP) (Fig.4). The counting line starts at the centre of sample U8 and ends at the top of sample U32. Thus, the top end of the greyscale record should correspond to U-series age U8 and the lower end to within the uncertainty of U32. Counting from the top we find 221 layers between the two end points at 396 and 617 years BP, i.e., the top counted age is only marginally younger, and the lower counted age is 43 years older compared to the U-series dates (c. 7% difference between both ages). This mismatch between the U/Th chronology and the greyscale-based layer counting probably results from uncertainties in the layer counting and characteristics of the greyscale profile. Whereas the layers are strongly pronounced in most of the profile, the interval between 32mm to 30.5mm (Fig.4) is accompanied by reduced growth rates and lower grey values, making it difficult to identify layers correctly.

For the KRUM-3 section, layers were counted for the past 5400 years. Repeated counting suggests that the overall disagreement between U/Th and counting chronologies is <5% (Breitenbach, 2009). Overall, the accordance between the two chronologies reveals the usefulness of layer counting based on grey values. The layer counting (c.5400 years) replaced the U-series chronology of the top half of stalagmite KRUM-3 covering the entire Holocene (Breitenbach, 2009). This improved the final chronology for the entire multiproxy record (i.e., grey values, stable isotopes, and elements) and gave new insights into teleconnections between the Indian summer monsoon and the Pacific climate (ENSO) (Breitenbach, 2009).

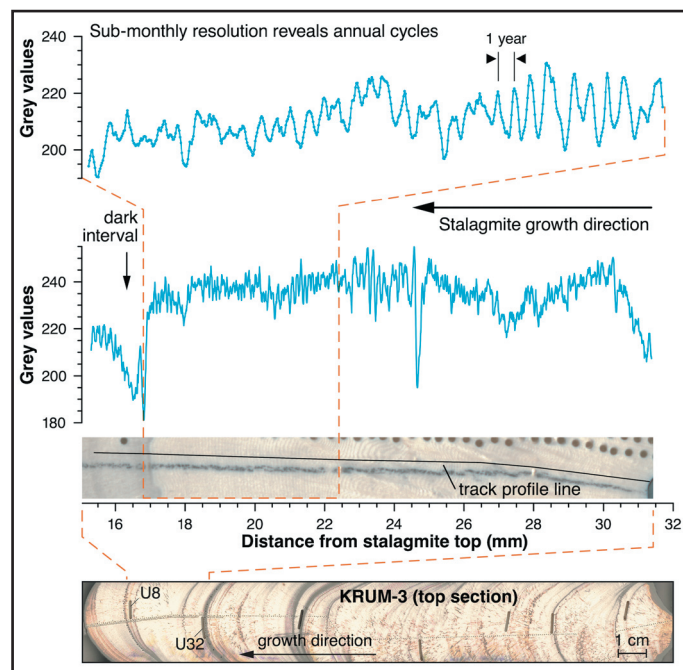


Figure 4: A section from stalagmite KRUM-3 shows annual laminae. Its greyscale values vary between 180 and 255. The high spatial resolution and high stalagmite growth rate result in sub-monthly temporal resolution (15 to 20 samples/year). Grey values drop to a minimum of around 180 during a low growth interval (dark interval); similarly low values are found in a hole at 24.6mm. The counting error in such dark low-growth intervals is certainly higher, because the layers become ill-defined. Annual cycles are clearly distinguishable in the zoomed section. A growth year has been defined as the interval between successive grey value maxima.

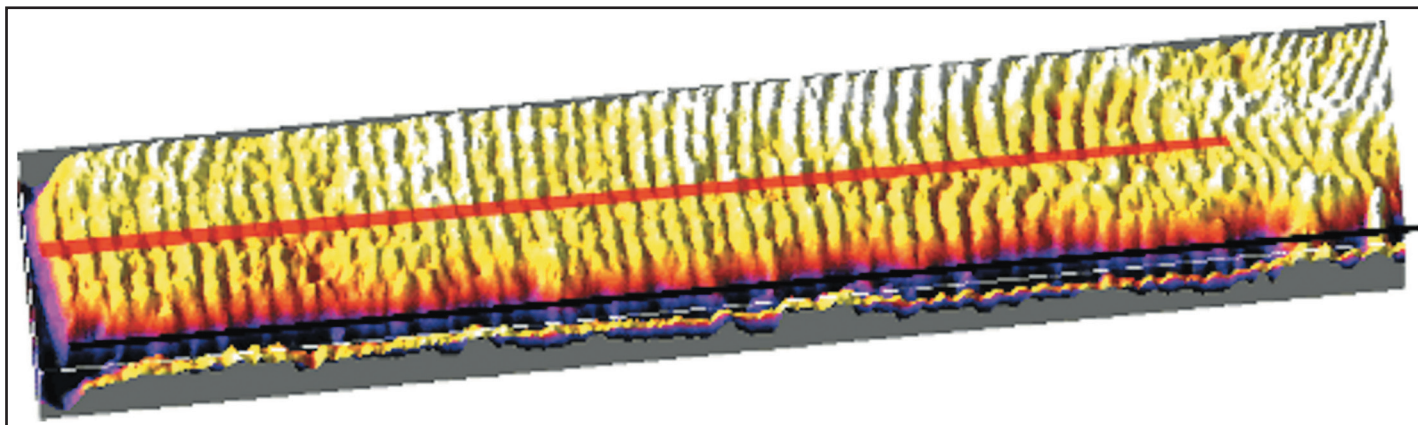


Figure 5: Plotting a grey value profile of a selected area using the Interactive 3D Surface Plot plugin. The block image can be rotated, and parameters can be customized in ImageJ before export of the final image. Annual layers (the growth direction is from right to left) are clearly visible.

The disagreement between the two independent dating methods also highlights the limitations of layer counting as a chronological tool, and careful examination is required to avoid underestimation and overestimation of ages in layer-counted chronologies (Shen *et al.*, 2013).

It must be emphasized that the subjectivity in counting individual layers leads to a human bias during data acquisition. Subjective selection of the maximum or minimum grey values in a given year is unavoidable where counting is complicated by irregular layer thinning or even fading of layers in low-growth intervals (as for example between 16mm to 18mm from the top in KRUM-3, Fig.4). As mentioned above, such intervals are particularly prone to increased counting uncertainties. Where clear and parallel laminae are visible the error is likely to be tiny and different users will obtain the same counting results (e.g., 20mm to 22mm from top in KRUM-3, Fig.4). Automated methods are potentially faster and give robust and objective results, but likewise these need special controlling steps, because some features in the sample might remain undetected by any automated method (e.g., Meyer *et al.*, 2006; Ebert and Trauth, 2015; Sliwinski *et al.*, 2023).

The layer-counting method is especially useful for establishing chronologies in cases where U/Th dating shows large errors, caused for example by low uranium or high detrital thorium contents. An exciting prospect is the extraction of sub-annual greyscale information from stalagmites that are too old for highly accurate U/Th chronologies to be obtained. Even under ideal conditions, U/Th dates from samples older than approximately 200,000 years probably have 2σ uncertainties of several hundred years (Cheng *et al.*, 2013). If layers can be counted in such samples, floating, yet internally highly precise, layer-counting chronologies can give insights into changes in seasonality, short-lived extreme events, or sub-decadal- to sub-centennial-scale environmental dynamics (e.g., Hopley *et al.*, 2018; Finestone *et al.*, 2022).

Data visualization

The information from the processed greyscale dataset can be presented either as an age–depth plot (using the layer-counting information) or as time series of grey values (using the composite record). The former is important when evaluating growth-rate dynamics and whether layer-counted intervals correspond with independent dating information. In many cases the latter is the final product that palaeoclimatologists interpret in terms of past environmental changes. Commonly it is useful to show the time series with its confidence interval, although this visualization depends upon the research aims.

In addition to exploiting greyscale data for chronological or proxy information, 2.5D (pseudo-3D) block diagrams can be used to visualize fabric characteristics of a speleothem sample. Such diagrams can be produced using the ImageJ Interactive 3D Surface Plot plugin (Plugins > 3D), which is installed by default with ImageJ.

An interactive tool can be used to enhance the greyscale information of a selected area of interest within a stalagmite. Various options help to highlight the selected surface in 3D, where the z-axis will be represented by the greyscale data. An example is given in Figure 5. Unfortunately, no measurement options are available in this toolbox, or for images saved from the 3D tool. The advantage of plotting greyscale data in 3D space is the opportunity to investigate and accentuate diffuse changes within the speleothem. This tool is also especially helpful during data acquisition because it aids identification of representative growth patterns, disturbed areas, or holes.

Conclusions

We present an overview on the usage of the freely available software ImageJ as a tool for the extraction of greyscale information from stalagmites (and possibly other laminated sediments). Stalagmite greyscale data obtained with this software can be exploited as (i) a proxy record in case the grey intensity is related to crystallography, growth rate or organic content changes of the stalagmite, which themselves depend upon environmental dynamics, and (ii) as a means to establish a layer-counting chronology if the grey values show clear seasonal cycles.

Independent absolute time markers are needed to verify that cycles found in the greyscale profile are indeed seasonal. The computer scripts provided allow for the concatenation of individual grey value tracks and for interpolation between absolute datings or counted peaks. Furthermore, this latter script also estimates the uncertainty of the chronology of the record obtained. Lastly, an example of greyscale analysis on a stalagmite is given. Analogously, the ImageJ program, the scripts, and the described methods can be used for other sediments (ice, lacustrine, and marine cores). We hope that the presented analytical strategies will be of use to readers interested in extracting high-resolution data from stalagmites without the need for the high funding levels that are commonly required to support provision of detailed geochemical analyses.

Data and code availability

We provide three scripts for MATLAB and Octave to extract grey values from scanned images (`extract_greyvalues.m`), to concatenate grey value tracks (`combine_tracks.m`), and for interpolation and uncertainty estimation of the grey value record (`chronology_with_uncert.m`). Use of Octave was tested with version 6.2.0 and of MATLAB with version 2023. The scripts with description and used data examples are available at Zenodo doi:10.5281/zenodo.7963381.

Acknowledgements

This work was supported by the German Research Foundation DFG (project MA 4759/18-1). Also, we thank two anonymous pre-reviewers who agreed that our initial draft was worth developing for submission to *Cave and Karst Science*, and provided many helpful suggestions. Bryce Belanger and Philip Hopley are thanked for their thorough and insightful reviews, both of which helped to improve our final manuscript.

References

- Aharon, P, Rasbury, M and Murgulet, V, 2006. Caves of Niue Island, South Pacific: Speleothems and water geochemistry. In *Perspectives on Karst Geomorphology, Hydrology, and Geochemistry – A Tribute Volume to Derek C Ford and William B White*. [Geological Society of America.] [https://doi.org/10.1130/2006.2404(24)]
- Baker, A, Barnes, W and Smart, P L, 1996. Speleothem luminescence intensity and spectral characteristics: Signal calibration and a record of palaeovegetation change. *Chemical Geology*, Vol.130, 65–76. [https://doi.org/10.1016/0009-2541(96)00003-4]
- Baker, A, Smith, C, Jex, C, Fairchild, I, Genty, D and Fuller, L, 2008. Annually laminated speleothems: a review. *International Journal of Speleology*, Vol.37, 193–206. [https://digitalcommons.usf.edu/ijss/vol37/iss3/4/]
- Baker, A, Smart, P L, Lawrence Edwards, R and Richards, D A, 1993. Annual growth banding in a cave stalagmite. *Nature*, Vol.364, 518–520. [https://doi.org/10.1038/364518a0]
- Baldini, J U, Lechleitner, F A, Breitenbach, S F, van Hunen, J, Baldini, L M, Wynn, P M, Jamieson, R A, Ridley, H E, Baker, A J, Walczak, I W and Fohlmeister, J, 2021. Detecting and quantifying palaeoseasonality in stalagmites using geochemical and modelling approaches. *Quaternary Science Reviews*, Vol.254, 106784. [https://doi.org/10.1016/j.quascirev.2020.106784]
- Balic, N and Koch, B, 2009. Canscan – An Algorithm for Automatic Extraction of Canyons. *Remote Sensing*, Vol.1, 197–209. [https://doi.org/10.3390/rs1030197]
- Boch, R, Spötl, C and Frisia, S, 2011. Origin and palaeoenvironmental significance of lamination in stalagmites from Katerloch Cave, Austria. *Sedimentology*, Vol.58, 508–531. [https://doi.org/10.1111/j.1365-3091.2010.01173.x]
- Boës, X and Fagel, N, 2008. Relationships between southern Chilean varved lake sediments, precipitation and ENSO for the last 600 years. *Journal of Paleolimnology*, Vol.39, 237–252. [https://doi.org/10.1007/s10933-007-9119-9]
- Breitenbach, S F, 2009. Changes in Monsoonal Precipitation and Atmospheric Circulation During the Holocene Reconstructed from Stalagmites from Northeastern India. *PhD thesis*, University of Potsdam. [https://doi.org/10.2312/GFZ.b103-10060]
- Breitenbach, S F M, Rehfeld, K, Goswami, B, Baldini, J U L, Ridley, H E, Kennett, D, Pruffer, K, Aquino, V V, Asmerom, Y, Polyak, V J, Cheng, H, Kurths, J and Marwan, N, 2012. COntstructing Proxy-Record Age models (COPRA). *Climate of the Past*, Vol.8, 1765–1779. [https://doi.org/10.5194/cp-8-1765-2012]
- Cheng, H, Lawrence Edwards, R, Shen, C-C, Polyak, V J, Asmerom, Y, Woodhead, J, Hellstrom, J, Wang, Y, Kong, X, Spötl, C, Wang, X and Calvin Alexander, E, 2013. Improvements in ²³⁰Th dating, ²³⁰Th and ²³⁴U half-life values, and U–Th isotopic measurements by multi-collector inductively coupled plasma mass spectrometry. *Earth and Planetary Science Letters*, Vol.371–372, 82–91. [https://doi.org/https://doi.org/10.1016/j.epsl.2013.04.006]
- Dasgupta, S, Saar, M O, Edwards, R L, Shen, C-C, Cheng, H and Alexander, E C, 2010. Three thousand years of extreme rainfall events recorded in stalagmites from Spring Valley Caverns, Minnesota. *Earth and Planetary Science Letters*, Vol.300, 46–54. [https://doi.org/10.1016/j.epsl.2010.09.032]
- Divya, K and Kaur, S, 2021. A Study on Tree Rings: Dendrochronology using Image Processing. *IOP Conference Series: Materials Science and Engineering*, Vol.1022, 012115. [https://doi.org/10.1088/1757-899X/1022/1/012115]
- Domínguez-Villar, D, Baker, A, Fairchild, I J and Edwards, R L, 2012. A method to anchor floating chronologies in annually laminated speleothems with U–Th dates. *Quaternary Geochronology*, Vol.14, 57–66. [https://doi.org/10.1016/j.quageo.2012.04.019]
- Ebert, T and Trauth, M H, 2015. Semi-automated detection of annual laminae (varves) in lake sediments using a fuzzy logic algorithm. *Palaeogeography, Palaeoclimatology, Palaeoecology*, Vol.435, 272–282. [https://doi.org/10.1016/j.palaeo.2015.05.024]
- Fairchild, I and Baker, A, 2012. *Speleothem Science: from processes to past environments*. [Wiley-Blackwell.] 432pp. ISBN 978-1-4051-9620-8.
- Fairchild, I and McMillan, E, 2007. Speleothems as indicators of wet and dry periods. *International Journal of Speleology*, Vol.36, 69–74. [https://doi.org/10.5038/1827-806X.36.2.2]
- Fairchild, I J, Baker, A, Borsato, A, Frisia, S, Hinton, R W, McDermott, D and Tooth, A F, 2001. Annual to sub-annual resolution of multiple trace-element trends in speleothems, *Journal of the Geological Society*, Vol.158, 831–841. [https://doi.org/10.1144/jgs.158.5.831]
- Fairchild, I J, Smith, C L, Baker, A, Fuller, L, Spötl, C, Matthey, D, McDermott, F and E.I.M.F. [Edinburgh Ion Microprobe Facility], 2006. Modification and preservation of environmental signals in speleothems. *Earth-Science Reviews*, Vol.75, 105–153. [https://doi.org/10.1016/j.earscirev.2005.08.003]
- Finestone, E M, Breeze, P S, Breitenbach, S F M, Drake, N, Bergmann, L, Maksudov, F, Muhammadiyev, A, Scott, P, Cai, Y, Khatsenovich, A M, Rybin, E P, Nehrke, G, Boivin, N and Petraglia, M, 2022. Paleolithic occupation of arid Central Asia in the Middle Pleistocene. *PLOS ONE*, Vol.17, 1–31. [https://doi.org/10.1371/journal.pone.0273984]
- Fischer, M, Botz, R, Schmidt, M, Rockenbauch, K, Garbe-Schönberg, D, Glodny, J, Gerling, P and Littke, R, 2006. Origins of CO₂ in Permian carbonate reservoir rocks (Zechstein, Ca₂) of the NW-German Basin (Lower Saxony). *Chemical Geology*, Vol.227, 184–213. [https://doi.org/10.1016/j.chemgeo.2005.09.014]
- Frisia, S, 2015. Microstratigraphic logging of calcite fabrics in speleothems as tool for palaeoclimate studies, *International Journal of Speleology*, Vol.44, 1–16. [https://doi.org/10.5038/1827-806X.44.1.1]
- Frisia, S, Borsato, A, Susini, J and Somogyi, A, 2005. Climate forcings and their influence on alpine history as reconstructed through the application of synchrotron-based X-ray microfluorescence on layered stalagmites. *Archaeometry*, Vol.47, 209–219. [https://doi.org/10.1111/j.1475-4754.2005.00197.x]
- Frisia, S, Borsato, A, Hartland, A, Faraji, M, Demeny, A, Drysdale, R N and Marjo, C E, 2022. Crystallization pathways, fabrics and the capture of climate proxies in speleothems: Examples from the tropics. *Quaternary Science Reviews*, Vol.297, 107833. [https://doi.org/10.1016/j.quascirev.2022.107833]
- Gabitov, R I, Watson, E B and Sadekov, A, 2012. Oxygen isotope fractionation between calcite and fluid as a function of growth rate and temperature: An in situ study. *Chemical Geology*, Vol.306–307, 92–102. [https://doi.org/10.1016/j.chemgeo.2012.02.021]
- Genty, D and Quinif, Y, 1996. Annually Laminated Sequences in the Internal Structure of Some Belgian Stalagmites – Importance for Paleoclimatology. *SEPM Journal of Sedimentary Research*, Vol.66. [https://doi.org/10.1306/D426831A-2B26-11D7-8648000102C1865D]
- Henderson, G M, 2006. Caving In to New Chronologies, *Science*, Vol.313, 620–622. [https://doi.org/10.1126/science.1128980]
- Hopley, P J, Weedon, G P, Brierley, C M, Thrasivoulou, C, Herries, A I R, Dinckal, A, Richards, D A, Nita, D C, Parrish, R R, Roberts, N M W, Sahy, D and Smith, C L, 2018. Orbital precession modulates interannual rainfall variability, as recorded in an Early Pleistocene speleothem. *Geology*, Vol.46, 731–734. [https://doi.org/10.1130/G45019.1]
- Ishino, T, Boisson, B, Orito, Y, Lacroix, C, Bischoff, E, Loussert, C, Janse, C, Ménard, R., Yuda, M and Baldacci, P, 2009. LISP1 is important for the egress of *Plasmodium berghei* parasites from liver cells. *Cellular Microbiology*, Vol.11, 1329–1339. [https://doi.org/10.1111/j.1462-5822.2009.01333.x]
- Jex, C N, Baker, A, Fairchild, I J, Eastwood, W J, Leng, M J, Sloane, H J, Thomas, L and Bekaröglu, E, 2010. Calibration of speleothem δ¹⁸O with instrumental climate records from Turkey. *Global and Planetary Change*, Vol.71, 207–217, 110. [https://doi.org/10.1016/j.gloplacha.2009.08.004]
- Johnson, K R, Hu, C, Belshaw, N S and Henderson, G M, 2006. Seasonal trace-element and stable-isotope variations in a Chinese speleothem: The potential for high-resolution paleomonsoon re-construction. *Earth and Planetary Science Letters*, Vol.244, 394–407.
- Kennett, D J, Breitenbach, S F M, Aquino, V V, Asmerom, Y, Awe, J, Baldini, J U L, Bartlein, P, Culleton, B J, Ebert, C, Jazwa, C, Macri, M J, Marwan, N, Polyak, V, Pruffer, K M, Ridley, H E, Sodemann, H, Winterhalder, B and Haug, G H, 2012. Development and Disintegration of Maya Political Systems in Response to Climate Change. *Science*, Vol.338, 788–791. [https://doi.org/10.1126/science.1226299]
- Kwiecien, O, Braun, T, Brunello, C F, Faulkner, P, Hausmann, N, Helle, G, Hoggarth, J A, Ionita, M, Jazwa, C, Kelmelis, S, Marwan, N, Nava-Fernandez, C, Nehme, C, Opel, T, Oster, J L, Perşoiu, A, Petrie, C, Pruffer, K, Saarni, S M, Wolf, A and Breitenbach, S F M, 2022. What we talk about when we talk about seasonality – A transdisciplinary review. *Earth-Science Reviews*, Vol.225, 103843. [https://doi.org/10.1016/j.earscirev.2021.103843]
- Louys, J, Duval, M, Price, G J, Westaway, K, Zaim, Y, Rizal, Y, Puspangrum, M, Trihascaryo, A, Breitenbach, S F M, Kwiecien, O, Cai, Y, Higgins, P, Albers, P C H, de Vos, J and Roberts, P, 2022. Speleological and environmental history of Lida Ajer cave, western Sumatra. *Philosophical Transactions of the Royal Society B: Biological Sciences*, Vol.377, [https://doi.org/10.1098/rstb.2020.0494]

- Mangili, C, Brauer, A, Plessen, B and Moscarriello, A, 2007. Centennial-scale oscillations in oxygen and carbon isotopes of endogenic calcite from a 15,500 varve year record of the Piànico interglacial. *Quaternary Science Reviews*, Vol.26, 1725–1735. [<https://doi.org/10.1016/j.quascirev.2007.04.012>]
- Marwan, N, Trauth, M H, Vuille, M and Kurths, J, 2003. Comparing modern and Pleistocene ENSO-like influences in NW Argentina using nonlinear time series analysis methods. *Climate Dynamics*, Vol.21, 317–326. [<https://doi.org/10.1007/s00382-003-0335-3>]
- McCarroll, D, Pettigrew, E, Luckman, A, Guibal, F and Edouard, J-L, 2002. Blue Reflectance Provides a Surrogate for Latewood Density of High-latitude Pine Tree Rings. *Arctic, Antarctic, and Alpine Research*, Vol.34, 450–453. [<https://doi.org/10.1080/15230430.2002.12003516>]
- McDermott, F, 2004. Palaeo-climate reconstruction from stable isotope variations in speleothems: a review. *Quaternary Science Reviews*, Vol.23, 901–918. [<https://doi.org/10.1016/j.quascirev.2003.06.021>]
- McGarry, S F and Baker, A, 2000. Organic acid fluorescence: applications to speleothem palaeoenvironmental reconstruction. *Quaternary Science Reviews*, Vol.19, 1087–1101. [[https://doi.org/10.1016/S0277-3791\(99\)00087-6](https://doi.org/10.1016/S0277-3791(99)00087-6)]
- McGlynn, I, McSween, H and Fedo, C, 2008. Textural and chemical evidence of hydrodynamic sorting in sediments in Gusev Crater. In: *39th Annual Lunar and Planetary Science Conference*, Vol.1391, 1332.
- Meyer, M C, Faber, R and Spötl, C, 2006. The WinGeol Lamination Tool: new software for rapid, semi-automated analysis of laminated climate archives. *The Holocene*, Vol.16, 753–761. [<https://doi.org/10.1191/0959683606h1969rr>]
- Myers, C G, Oster, J L, Sharp, W D, Bennartz, R, Kelley, N P, Covey, A K and Breitenbach, S F, 2015. Northeast Indian stalagmite records Pacific decadal climate change: Implications for moisture transport and drought in India. *Geophysical Research Letters*, Vol.42, 4124–4132. [<https://doi.org/10.1002/2015GL063826>]
- Nederbragt, A and Thurow, J, 2001. A 6000 yr varve record of Holocene climate in Saanich Inlet, British Columbia, from digital sediment colour analysis of ODP Leg 169S cores. *Marine Geology*, Vol.174, 95–110. [[https://doi.org/10.1016/S0025-3227\(00\)00144-4](https://doi.org/10.1016/S0025-3227(00)00144-4)]
- Niggemann, S, Mangini, A, Mudelsee, M, Richter, D K and Wurth, G, 2003. Sub-Milankovitch climatic cycles in Holocene stalagmites from Sauerland, Germany. *Earth and Planetary Science Letters*, Vol.216, 539–547. [[https://doi.org/10.1016/S0012-821X\(03\)00513-2](https://doi.org/10.1016/S0012-821X(03)00513-2)]
- Oriani, F, Treble, P C, Baker, A and Mariethoz, G, 2022. WICount: Geological lamination detection and counting using an image analysis approach. *Computers and Geosciences*, Vol.160, 105 037. [<https://doi.org/10.1016/j.cageo.2022.105037>]
- Ozken, I, Eroglu, D, Stemler, T, Marwan, N, Bagci, G B and Kurths, J, 2015. Transformation-cost time-series method for analyzing irregularly sampled data. *Physical Review E*, Vol.91, 062911. [<https://doi.org/10.1103/PhysRevE.91.062911>]
- Patterson, R T, Prokoph, A, Reinhardt, E and Roe, H M, 2007. Climate cyclicity in late Holocene anoxic marine sediments from the Seymour–Belize Inlet Complex, British Columbia. *Marine Geology*, Vol.242, 123–140. [<https://doi.org/10.1016/j.margeo.2007.04.003>]
- Pike, J and Kemp, A E S, 1996. Preparation and analysis techniques for studies of laminated sediments, *Geological Society, London, Special Publications*, Vol.116, 37–48. [<https://doi.org/10.1144/GSL.SP.1996.116.01.05>]
- Raffi, I, Backman, J and Pälike, H, 2005. Changes in calcareous nannofossil assemblages across the Paleocene/Eocene transition from the paleo-equatorial Pacific Ocean. *Palaeogeography, Palaeoclimatology, Palaeoecology*, Vol.226, 93–126. [<https://doi.org/10.1016/j.palaeo.2005.05.006>]
- Rasband, W, 1997–2004. *ImageJ*. National Institutes of Health, Bethesda, Maryland, USA. [<http://rsb.info.nih.gov/ij/>]
- Regent Instruments Inc. WinDENDRO. [https://www.regentinstruments.com/assets/windendro_about.html]
- Rehfeld, K, Marwan, N, Heitzig, J and Kurths, J, 2011. Comparison of correlation analysis techniques for irregularly sampled time series. *Nonlinear Processes in Geophysics*, Vol.18, 389–404. [<https://doi.org/10.5194/npg-18-389-2011>]
- Ridley, H E, Asmerom, Y, Baldini, J U L, Breitenbach, S F M, Aquino, V V, Prufer, K M, Culleton, B J, Polyak, V, Lechleitner, F A, Kennett, D J, Zhang, M, Marwan, N, Macpherson, C G, Baldini, L M, Xiao, T, Peterkin, J L, Awe, J and Haug, G H, 2015. Aerosol forcing of the position of the intertropical convergence zone since ad 1550. *Nature Geoscience*, Vol.8, 195–200. [<https://doi.org/10.1038/ngeo2353>]
- Riechelmann, D F, Fohlmeister, J, Kluge, T, Jochum, K P, Richter, D K, Deininger, M, Friedrich, R, Frank, N and Scholz, D, 2019a. Evaluating the potential of tree-ring methodology for cross-dating of three annually laminated stalagmites from Zoolithencave (SE Germany). *Quaternary Geochronology*, Vol.52, 37–50. [<https://doi.org/10.1016/j.quageo.2019.04.001>]
- Riechelmann, S, Breitenbach, S F M, Schroeder-Ritzrau, A, Mangini, A, and Immenhauser, A, 2019b. Ventilation and cave air pCO₂ in the Bunker-Emst-Cave System (NW Germany): Implications for speleothem proxy data. *Journal of Cave and Karst Studies*, Vol.81, 98–112. [<https://doi.org/10.4311/2018ES0110>]
- Rodbell, D T, Seltzer, G O, Anderson, D M, Abbott, M B, Enfield, D B and Newman, J H, 1999. An ~15,000-Year Record of El Niño-Driven Alluviation in Southwestern Ecuador. *Science*, Vol.283, 516–520. [<https://doi.org/10.1126/science.283.5401.516>]
- Ronay, E R, Breitenbach, S F M and Oster, J L, 2019. Sensitivity of speleothem records in the Indian Summer Monsoon region to dry season infiltration. *Scientific Reports* 9:5091. [<https://doi.org/10.1038/s41598-019-41630-2>]
- Schiøtt, M, De Fine Licht, H H, Lange, L and Boomsma, J J, 2008. Towards a molecular understanding of symbiont function: Identification of a fungal gene for the degradation of xylan in the fungus gardens of leaf-cutting ants. *BMC Microbiology*, Vol.8, 40. [<https://doi.org/10.1186/1471-2180-8-40>]
- Scholz, D and Hoffmann, D L, 2011. StalAge – An algorithm designed for construction of speleothem age models. *Quaternary Geochronology*, Vol.6, 369–382. [<https://doi.org/10.1016/j.quageo.2011.02.002>]
- Shen, C-C, Lin, K, Duan, W, Jiang, X, Partin, J W, Edwards, R L, Cheng, H and Tan, M, 2013. Testing the annual nature of speleothem banding. *Scientific Reports*, Vol.3, 2633. [<https://doi.org/10.1038/srep02633>]
- Shopov, Y Y, Ford, D C and Schwarcz, H P, 1994. Luminescent microbanding in speleothems: High-resolution chronology and paleoclimate. *Geology*, Vol.22, 407. [[https://doi.org/10.1130/0091-7613\(1994\)022<0407:LMISHR>2.3.CO;2](https://doi.org/10.1130/0091-7613(1994)022<0407:LMISHR>2.3.CO;2)]
- Sliwinski, J, Mandl, M and Stoll, H, 2023. Machine learning application to layer counting in speleothems. *Computers and Geosciences*, Vol.171, 105287. [<https://doi.org/10.1016/j.cageo.2022.105287>]
- Smith, C L, Fairchild, I J, Spötl, C, Frisia, S, Borsato, A, Moreton, S G and Wynn, P M, 2009. Chronology building using objective identification of annual signals in trace element profiles of stalagmites. *Quaternary Geochronology*, Vol.4, 11–21. [<https://doi.org/10.1016/j.quageo.2008.06.005>]
- Thomas, E K and Briner, J P, 2009. Climate of the past millennium inferred from varved proglacial lake sediments on northeast Baffin Island, Arctic Canada. *Journal of Paleolimnology*, Vol.41, 209–224. [<https://doi.org/10.1007/s10933-008-9258-7>]
- Treble, P, Chappell, J and Shelley, J, 2005. Complex speleothem growth processes revealed by trace element mapping and scanning electron microscopy of annual layers. *Geochimica et Cosmochimica Acta*, Vol.69, 4855–4863. [<https://doi.org/10.1016/j.gca.2005.06.008>]
- Webster, J W, Brook, G A, Railsback, L B, Cheng, H, Edwards, R L, Alexander, C and Reeder, P P, 2007. Stalagmite evidence from Belize indicating significant droughts at the time of Preclassic Abandonment, the Maya Hiatus, and the Classic Maya collapse. *Palaeogeography, Palaeoclimatology, Palaeoecology*, Vol.250, 1–17. [<https://doi.org/10.1016/j.palaeo.2007.02.022>]
- Wong, C I and Brecker, D O, 2015. Advancements in the use of speleothems as climate archives. *Quaternary Science Reviews*, Vol.127, 1–18. [<https://doi.org/10.1016/j.quascirev.2015.07.019>]